Environmental Science and Pollution Research (2022) 29:71217–71231
https://doi.org/10.1007/s11356-022-20680-6

RESEARCH ARTICLE

Experimental evaluation of a solar-driven adsorption desalination system using solid adsorbent of silica gel and hydrogel

Mostafa Zarei Saleh Abad[1,2] · Mohammad Behshad Shafii[1,2] · Benyamin Ebrahimpour[1,3]

Received: 20 January 2022 / Accepted: 3 May 2022 / Published online: 21 May 2022

Abstract

Nowadays, the world is facing a shortage of fresh water. Utilizing adsorbent materials to adsorb air moisture is a suitable method for producing freshwater, especially combining the adsorption desalination system with solar energy devices such as solar collectors. The low temperature of solar collectors has caused some water to remain in the adsorbents in the desorption process and has reduced the possibility of using these systems. In this research, for the first time, an evacuated tube collector (ETC) is used as an adsorbent bed so that the temperature of the desorption process reaches higher values and as a result, more fresh water is expected to produced. In this study, two adsorption desalination systems (ADS) are experimentally investigated. In the first system, a laboratory experimental setup using silica gel and hydrogel adsorbents is used to investigate freshwater production using each of the two adsorbents. The effect of different parameters such as variable adsorption and desorption time, variable temperature and humidity of inlet air, and variable adsorbent mesh sizes on the desalination process is evaluated. Then, in the second system, an innovative configuration of the solar-driven adsorption desalination system with an ETC full of silica gel is studied. In the laboratory experimental setup, the maximum amount of water produced by silica gel is 0.36 L/kg and by hydrogel is 0.58 L/kg. In the solar-driven adsorption desalination system, the largest amount of accumulated water production, daily efficiency, and cost per liter (CPL) of produced water are 1.518 kg/m^2 day, 11.25%, and 0.0699 $/L, respectively. Therefore, this new configuration for an adsorption desalination system seems feasible.

Keywords Adsorption desalination · Silica gel · Hydrogel · Evacuated tube collector · Solar energy

Introduction

Desalination systems have become critically important because of limited freshwater resources (Salehi et al. 2020). However, these systems consume a great deal of electrical energy which is generated by fossil fuels. Utilizing renewable energy sources such as solar and wind energy can decline fossil fuel consumption (Akbar et al. 2019). These days, different desalination processes are used, one of the most important of which is adsorption desalination (Youssef et al. 2014). Due to the high volume of vapor in many parts of the world, these desalination systems have attracted a lot of attention. These systems can produce freshwater by adsorbing air moisture and then excreting it under certain conditions. Adsorbents are usually solid hydrophilic materials with high degrees of porosity (Youssef et al. 2015). Silica gel and zeolite are also mostly used as solid adsorbents. Two of the most important moisture-absorbent liquid materials are LiCl and $CaCl_2$ (Jamil and Ali 2019). The use of solid adsorbents such as silica gel has received much attention due to the lack of corrosion damage in desalination systems (Youssef et al. 2015). As a result, a great deal of research has been done on adsorption desalination systems using silica gel (Rahimi-ahar et al. 2020). Amirfakhraei et al. (2020) used a thermodynamic-mathematical model to investigate a two-bed adsorption desalination system with new heat and mass recovery cycle. The results were in good agreement with experimental data provided by Alsaman et al. (2017). The daily water production was 9.58 m^3/ton silica gel day,

Responsible editor: Philippe Garrigues

✉ Mohammad Behshad Shafii
behshad@sharif.edu

[1] Department of Mechanical Engineering, Sharif University of Technology, Tehran, Iran

[2] Sharif Energy, Water and Environment Institute (SEWEI), Tehran, Iran

[3] School of Mathematics and Physics, University of Portsmouth, Portsmouth, UK

which was about 66% more than the amount produced by the common adsorption systems with two beds. Sadri et al. (2018) studied an adsorption desalination system with heat and mass recovery employing a thermo-economic model. The optimal energy efficiency of the system and the cost of water production were 9.5% and 0.57 $/m^2, respectively. Ashraf et al. (2021), in a review study, elaborated on water vapor adsorption by metal–organic frameworks and mentioned different models of adsorption equilibrium equations used in the literature for adsorption isotherms data fitting.

The adsorption desalination systems have usually been combined with other processes. In an experimental study, Wang and Ng (2005) investigated an adsorption desalination system using low-temperature waste heat. The water produced by a 4-bed adsorption desalination system was 4.7 L/kg silica gel, which also could increase by rising temperature in the evaporator, or decrease the temperature in the cool water of the adsorption bed. Qasem and Zubair (2019) investigated the performance of a new AD/HDH system and compared it in two modes. A finned pipe heat exchanger and pre-cooled evaporator pipe were used before feeding with the HDH system. Seawater was used to cool the adsorption process in the second mode. The GOR, cost, and water production were 7.6–7.8, 6.4–6.5 $/m^2, and 25.30 kg/h, respectively. Capocelli et al. (2018) studied an HDHA system in which the HDH system was closed-water closed-air, based on a mathematical model. The results revealed GOR, RR, and the freshwater production of the system were 7, 7, and 30 m^3/day respectively. Elbassoussi et al. (2020) introduced a new hybrid AD/HDH system that simultaneously produced water and cooling power, using PV panels and natural gas as energy sources. COP, GOR, water production, and system cooling capacity were 0.46, 2.5, 21.75 kg/h, and 2.53 kW, respectively.

Hydrogels which are also compelling moisture-adsorbent materials are used in different desalination applications according to their types. In a review study, Salehi et al. (2020) mentioned various hydrogels in desalination plants such as solar still, FO, electro-dialysis, and capacitive desalination. The hydrogel was classified based on the physical structure of ionic charge, production methods, particle size, physical–chemical bonding, and mechanical properties. Using hydrogel plates in freshwater production tends to be cheaper than other desalination processes. Suleimenov et al. (2017) used a heat-sensitive hydrogel and polyelectrolyte gel for the desalination process. First, the water-containing polyelectrolyte gel was exposed to a heat-sensitive hydrogel and then the hydrogel was exposed to heat, such as solar radiation, to complete the desalination process.

Solar energy, one of the most important renewable energy sources, is available anywhere, and it does not cost a considerable amount to benefit from this source (Khalid et al. 2021). Much research has been done on solar desalination systems, especially solar-driven adsorption desalination systems. Using a theoretical dynamic model, Alsaman et al. (2017) predicted the performance of an experimental solar-driven adsorption desalination-cooling system in Egyptian weather conditions. The investigation showed 0.45 of COP, an average cooling capacity of 110 W/kg, and 4 m^3/ton silica gel water production. This system contained 13.5 kg of silica gel placed in two adsorption beds. In addition, ETCs with an area of 4.5 m^2 were used to heat water which was used as the working fluid. Hot water entered the storage tank, and then it flowed into the adsorbent bed if the desorption process was needed. Based on Alsaman's system, Rezk et al. (2019) investigated a solar-driven adsorption cooling system with a mathematical model, in which radial movement optimizer (RMO) algorithm with cycle time optimization parameters, input hot water temperature, input cold water, and the water flow rate was considered. The results were compared with the experimental data and finally the optimum amount of COP, cooling capacity, and desalinated water were 0.961, 191 W/kg, and 6.9 m^3/ton silica gel, respectively. In another study, Kabeel et al. (2017) numerically investigated the performance of a hybrid HDH desalination system with an air adsorber system. The solar air collector was used in the desorption process in order to increase air temperature. The results showed that between 3.175 and 5.011 L/h water could be produced, with a daily COP of 3.636–4.392. Kabeel and Abdelgaied (2019) experimentally investigated a desiccant dehumidifier system with cut segmental silica gel baffles (weighing 4.5 kg per channel) and water cooling (DDSBWC). It was composed of two new DDSBWC configuration subsystems for air conditioning and freshwater production. ETC was used to heat water in this system, and a solar air collector was used to heat reactivation air. COP was 0.4–1.584, and the average dehumidification capacity was 0.3264 L/kg silica gel. The result indicated that the configuration was a great choice for hot and humid regions. Ji et al. (2007) introduced a new highly efficient water-selective composite adsorbent to produce water from the atmosphere by utilizing solar energy. The adsorption capacity of the new composites was 1.75 L/kg adsorbent and the water production capacity of a solar still system with this adsorbent was 1.2 kg/m^2. Essa et al. (2020) investigated an adsorption desalination system using silica gel with a neural-fuzzy inference system. The desalination system consisted of a double-slope half-cylindrical basin solar still, and 4 long fins. In this system, a 1.5-cm layer of silica gel weighing 1.5 kg was used and the optimum freshwater production was about 400 mL/m^2 and also the theoretical and experimental results were well matched. Using MATLAB, Mitra et al. (2014) investigated a solar-driven adsorption desalination system containing 5.6 kg of silica gel, which included 4 adsorbent beds and could work even by non-concentrating type solar collectors. Du et al. (2017) conducted a study on the optimal area of ETCs for adsorption desalination. In this system, there were

2 absorbent beds, and ETCs were used to heat water for the desorption cycle, and this hot water produced was stored in a hot water tank. This optimization was aimed for reducing the price of produced water by using the minimum auxiliary thermal energy and the ETCs. Ali et al. (2017) simulated a solar hybrid adsorption desalination-cooling system in TRANSYS and MATLAB in Egyptian weather conditions. This system contained ETCs, 2 storage hot water tanks, and 2 silica gel adsorbent beds. Inside each adsorbent bed, there was 6.75 kg of silica gel. As a result of the simulation, the specific water production was 10 m^3/ton of silica gel. Talaat et al. (2018) conducted an experimental and theoretical study with calcium chloride liquid absorbent to produce water from air humidity in Egypt. The process of absorbing moisture from the air was done during the night, and the moisture in the absorbents was converted to steam by solar energy during the day. Finally, this steam was converted into drinking water inside the condenser. Approximately 0.331–0.631 kg/m^2 of drinking water was produced by this system every day.

It is observed that solar-driven adsorption desalination systems in previous research utilized ETCs to use solar energy in the desorption process. However, the adsorbent beds were separated from the ETCs, and the working fluid (generally water) flowed inside the solar collectors to absorb heat. After absorbing heat, working fluid entered the hot water tank and was used to regenerate the adsorbents. In other studies that used solar still systems containing adsorbents, the maximum desorption temperature of adsorbents was at a low level, about 75 °C (Ji et al. 2007; Essa et al. 2020). According to Qiu et al. (2017), for the silica gel to dry completely, a temperature of about 150 °C is required. Therefore, the weakness of previous studies is that they did not reach this temperature level (150 °C) and as a result, the inside moisture of silica gel was not completely converted into steam. This study proposes an innovative configuration in which ETC is used as the adsorbent bed in which silica gel is poured. Silica gel is in direct contact with the tube wall. Therefore, the system is more compact than previous designs that had separate adsorption beds. Secondly, the temperature of silica gel is expected to reach higher temperatures than those of previous studies due to the direct contact between silica gel and the adsorbent bed (ETC). Compared to previous research, it is expected that the silica gel in this study to dry completely by reaching a higher temperature in the desorption process and most of the water inside the silica gel to be converted into steam. As a result, the water production of the system will increase. In point of fact, a novel automatic irrigation system is designed and built as a solar-driven adsorption desalination system with an ETC filled with silica gel. During the night, the system adsorbs and stores air moisture by adsorbent materials, and during the day, the desorption process occurs under sunlight. An ETC is used because it can reach a higher temperature in the desorption process. No research has investigated the role of using an ETC with silica gel directly on an adsorption desalination system to supply heating in the daytime. Two AD systems are experimentally investigated in this study. In the first system, to study silica gel and hydrogel behavior deeply, in the laboratory environment, these adsorbents are investigated with a laboratory experimental setup under different conditions. The experiment is designed to measure the ability of the adsorbents in storing moisture and producing freshwater. The effect of different parameters such as variable adsorption and desorption time, variable temperature and humidity of inlet air, and variable adsorbent mesh sizes on the desalination process is evaluated. In the second system, a solar-driven adsorption desalination system equipped with an ETC is studied. The second system is designed and manufactured for the first time as an automatic irrigation system to store moisture in adsorbent materials in hot and humid areas at night, where the air is slightly cold. Then, in the daytime, due to the warming adsorbents in the ETC, the air that passes through the adsorbents receives the moisture inside the adsorbents and then enters the condenser and turns into fresh water. Finally, the daily efficiency and economic parameters of the solar-driven adsorption desalination system are calculated, and the accumulated daily water production is compared to the other studies.

Experimental and Instrumentation

All of the experiments are carried out in Tehran, Iran (longitude: 51.38°E and latitude: 35.72°N and elevation: 1172 m). Two ADS systems are experimentally investigated. First, the laboratory experimental setup is tested in a laboratory environment. Then, the solar-driven adsorption desalination system is evaluated under solar irradiance to check the potential of this system on farms for automatic irrigation. Both of the systems include the first process (adsorption) and the second process (desorption). The details of each system are presented in the following sections.

Laboratory experimental setup

Figure 1 depicts a schematic of the laboratory experimental setup. According to this figure, in the adsorption process, the ambient air enters the glass box from inlet 1. Its relative humidity and temperature increase using an ultrasonic humidifier and heater 1. As a result, the moisture and temperature of the inlet air of the adsorbent material are adjusted. Then, utilizing a fan, the processed air is taken out of port 2, automatically, and sent to the chamber of heater 2. In the adsorption process, heater 2 is turned off and as a result the air with the same characteristics exits through point 4 and enters the water–vapor chamber. After separating

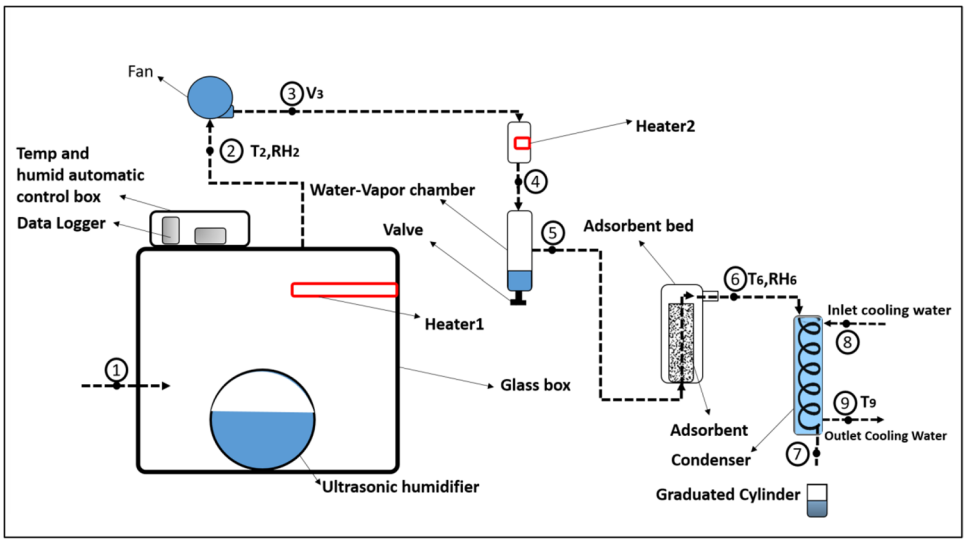

Fig. 1 Schematic view of the experimental unit during the adsorption and desorption processes

water droplets from the air in this chamber, the air exits through port 5 and reaches the adsorbent bed. The adsorbent bed contains an aluminum tube filled with the adsorbent material placed inside a glass container. Because the adsorption process is an exothermic reaction, the air temperature rises, but the humidity decreases during thermal and moisture exchange with the adsorbent. In the following, the air leaves the adsorbent bed and reaches the condenser inlet in point 6. The parallel flow condenser of this system is a heat exchanger with indirect contact. Air passes through the copper coil inside the condenser and exits the system through port 7. Meanwhile, cold water enters the condenser from point 8, and, after exchanging heat with the air inside the copper coil, leaves the condenser through point 9. In the desorption process, ambient air enters the glass box through port 1. In this process, the ultrasonic humidifier is off, and only heater 1 in the glass box is on. As air temperature rises, the processed air exits the glass box through port 2 with the help of the fan. Since more heat is needed to perform the desorption process, heater 2 is on in this process, and the air, after exchanging heat with heater 2 and increasing air temperature, exits through port 4 and enters the water–vapor chamber. After separating water droplets from the hot air, it leaves port 5 and enters the adsorbent bed. Since this desorption process is an endothermic reaction, after exchanging heat and moisture with adsorbent materials, the humidity of the hot air increases, and its temperature decreases. The air leaves the adsorbent bed through port 6 and enters the condenser and passes through the copper coil. As a result, the air transfers heat to the cold water inside the condenser, and the temperature of the passing air decreases and water droplets are formed. These droplets are collected in the graduated cylinder through port 7, which is located at the condenser outlet. The water–vapor chamber is installed to separate water from the air and prevent water droplets from reaching the adsorbent material. Therefore, only the moisture in the adsorbent is carried by air in the desorption process and converted into water.

Solar-driven adsorption desalination system

As shown in Fig. 2c, the solar-driven adsorption desalination system includes the same equipment as the laboratory experimental setup, just instead of heater 2, the adsorbent material inside the ETC is heated by the solar radiation in the desorption process. In addition, a counter-flow condenser is used in this system. Instead of a copper coil, an aluminum tube containing 300 g of aluminum filings is used, which is intended to create porosity inside the tube, as well as enhancing the heat transfer area and reducing air velocity. Since this system is used to adsorb moisture of the air at night in hot and humid regions and then produce water or automatic irrigation during the day, a glass box with a heater and ultrasonic humidifier is used to adjust the temperature and relative humidity of the inlet air. As mentioned in Fig. 1, the adsorption process takes place at night. In this process, first, ambient air enters the glass box through port 1, and its temperature and relative humidity increase by means of the heater and humidifier. Therefore, the inlet air is adjusted to the adsorbent process. This processed air is then taken out of the glass box through port 2 utilizing a fan, automatically, and goes into the water–vapor chamber. After separating water droplets from the air, the air exits the water–vapor chamber through point 4 and is conducted into the steel tube inside the ETC. According to Fig. 2b, the ETC is filled with silica gel and the steel tube is perforated at equal distances so that the air is directed through the holes to the adsorbent material while passing through the steel tube. Finally, after heat and humidity exchange with the adsorbent material, the air loses some moisture. Due to the exothermic reaction of

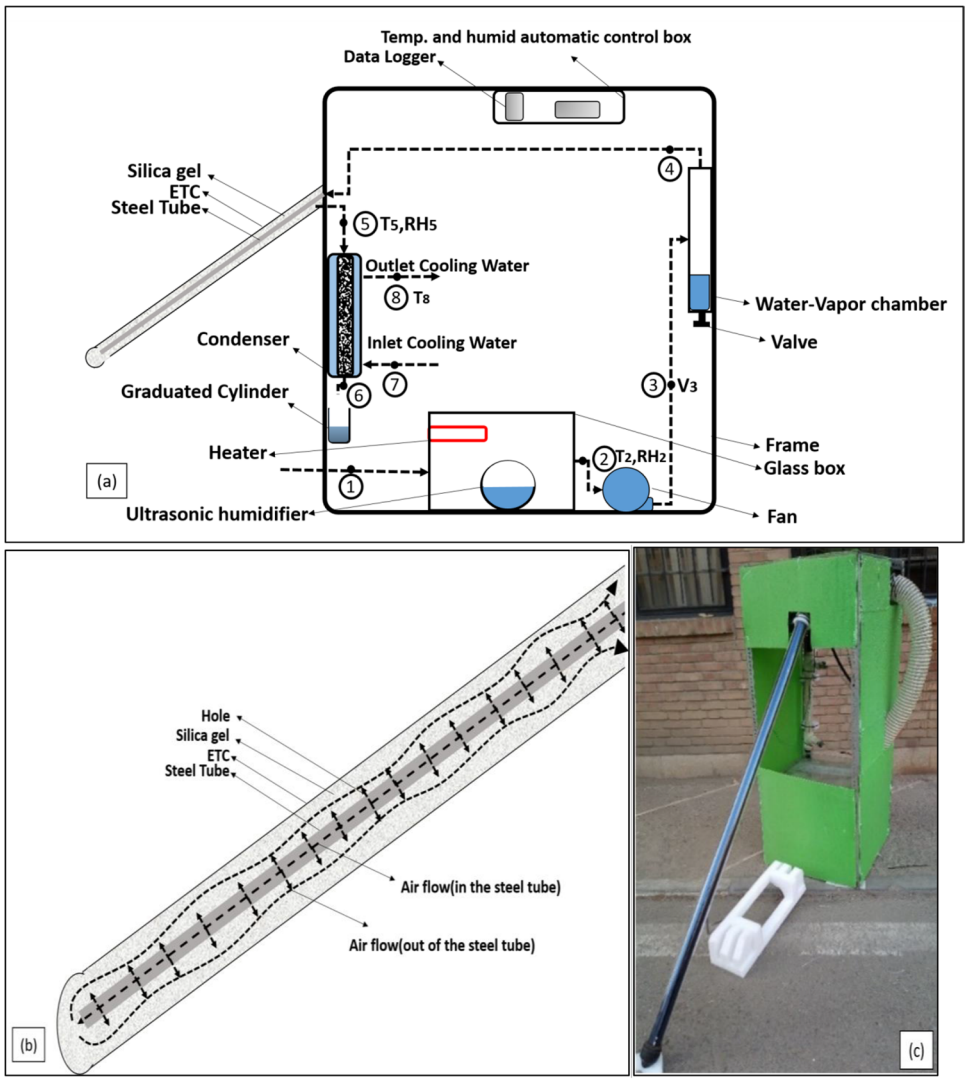

Fig. 2 **a** Schematic view of solar-driven adsorption desalination system during the adsorption and desorption processes, **b** airflow in ETC, and **c** solar-driven adsorption desalination system

the air and the adsorbent material in the adsorption process, the temperature of the air rises. Then, the airflow outside the steel tube is directed upwards and exits the collector through port 5. After that, air passes through the condenser and then exits the condenser through point 6. The desorption process begins with sunrise on the collector. In this process, the humidifier is turned off, and only the heater is on to enhance the temperature of inlet air from port 1 and adjust it to the glass box. Using a fan, this processed air exits through port 2 automatically and enters the water–vapor chamber. After the air passes through the water–vapor chamber through point 4, it reaches the collector. At this process, because the solar rays heat the adsorbent material and steel tube in the collector, heater 2 is not functional in this system, and the air is heated by passing through a steel tube. After passing through the holes on the steel tube, the air exchanges moisture and heat with the adsorbent, and its humidity rises. The desorption process is an endothermic reaction, but due to the fact that the temperature of the adsorbent material is high, the temperature of the air leaving the collector increases. This air exits the collector through port 5 and enters the condenser. In the condenser, the air contains a heat exchange with the water outside the tube after passing through the tube and aluminum filings and as a result air temperature decreases. Then, as the temperature decreases, water droplets form and exit the condenser through point 6 and are collected inside the graduated cylinder.

The specifications of the two systems are listed in Table1.

Characteristics of silica gel and hydrogel

Utilizing nitrogen gas at 77 K in the BET (Brunauer, Emmett, and Teller) test, adsorption and desorption of the adsorbents are measured and determined in Fig. 3a and b. Additionally, the size and dimensions of the pores of each adsorbent are precisely determined. In Fig. 3a and b, C_a is the adsorption isotherm capacity in liter per kilogram of adsorbent, plotted in terms of pressure (P/P_0), and the results

Table 1 Details of the dimensions and sizes of the equipment used

System 1 (component)	Specification	System 2 (component)	Specification
The heater 2	500 W	Evacuated tube collector	Outer diameter:57 mm Inner diameter: 47 mm Length: 1820 mm
Fan	4000 rpm	Fan	4000 rpm
–	–	Frame	$60\times60\times150$ cm^3
Humidifier	Height: 40 cm Diameter: 25 cm	Humidifier	Height: 40 cm Diameter: 25 cm
The heater 1	2000 W	The heater	2000 W
Glass box	$50\times50\times50$ cm^3	Glass box	$50\times50\times50$ cm^3
Water–vapor chamber	Length: 70 cm Diameter: 8 cm	Water–vapor chamber	Length: 80 cm Diameter: 12 cm
Adsorbent bed Aluminum tube	Diameter: 5 cm Length: 20 cm Diameter: 2 cm Length: 20 cm	Steel tube	Diameter: 10 mm Length: 180 cm
Condenser	diameter of copper coil: 12 mm steel tube with diameter of 20 cm and length of 50 cm	Condenser	Aluminum tube with diameter of 3 cm and length of 80 cm. 300 gr of aluminum filings, and PVC tube with diameter of 5 cm and a length of 60 cm

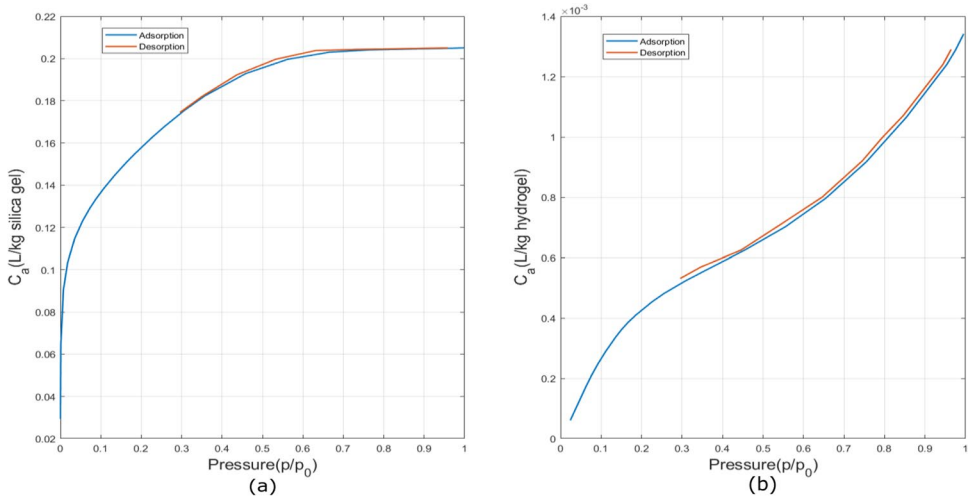

Fig. 3 **a** The adsorption and desorption isotherm capacity of silica gel in BET analysis. **b** The adsorption and desorption isotherm capacity of hydrogel in BET analysis

obtained have the same trend as previous research (Mohammed et al. 2018). In general, with increasing pressure, the adsorption capacity of silica gel inclines to a certain and limited number. In the hydrogel test, the adsorption capacity can be divided into two regions before and after P/P_0 equal to 0.5. The adsorption rate of the hydrogel before 0.5 has a trend almost similar to silica gel, and with increasing pressure, the adsorption capacity increases at a low rate. But for values above 0.5, with increasing P/P_0, the slope of the adsorption capacity is also much higher (Mittal et al. 2020). In other words, in the region of less than 0.5, the nitrogen pressure is low, and the nitrogen molecules are not capable of penetrating into the internal pores of the hydrogel, resulting in a lower adsorption capacity of the hydrogel. On the other hand, when P/P_0 is higher than 0.5, the inlet air pressure increases, the penetration of nitrogen molecules into the hydrogel adsorbent heightens, and gas reaches the internal pores of the adsorbent. As a result, the adsorption capacity of hydrogel will increase (Mittal et al. 2020).

Table 2 shows the characteristics of solid adsorbents using BET and BJH (Barrett-Joyner-Halenda) analysis. It is worth mentioning that the diameter and volume of the adsorbent pores are determined based on the BJH analysis. It is observed that the BET-specific surface area of silica gel and hydrogel adsorbents are 441.46 and 1.2211 m^2/gr, respectively, and also the total pore volume of silica gel is much larger than hydrogel. This means that the silica gel used in this study has much more porosity than the hydrogel. Therefore, the amount of nitrogen gas adsorption capacity of the silica gel is much higher, according to Fig. 3a and b. On the other hand, the hydrogel is considered a super adsorbent (Mittal et al. 2020) due to the very high adsorption of water vapor compared to silica gel. In other words, the adsorption and desorption figures of N_2 gas cannot be generalized to the adsorption and desorption capacity of water vapor isotherms. Nitrogen is a completely non-polar gas. It acts only on adsorption and desorption isotherms with the Van der Waals' model for interaction on solid adsorbents with the porosity surface (Mortimer 1983). In fact, the Van der Waals' bonds between nitrogen gas and silica gel are higher than the bonds between nitrogen gas and hydrogel due to the high porosity of silica gel, and it causes a higher adsorption capacity in the silica gel. While in a polar fluid such as water, special bonds such as hydrogen bonds play a key role (Mortimer 1983). The hydrogen bonds formed between hydrogel particles and water are expected to be much more and stronger than the hydrogen bonds between silica gel and water. As a result, despite having a smaller surface area of hydrogel compared to silica gel, the hydrogel performs exceptionally better in contact with water vapor due to its distinct type of interaction.

Table 2 Characteristics of studied solid adsorbents

Adsorbent	BET-specific surface area [m^2 gr^{-1}]	Mean pore diameter [nm]	Total pore volume [cm^3 gr^{-1}]	Pore specific surface area [m^2 gr^{-1}]
Hydrogel	1.2211	5.1674	0.0015	1.1262
Silica gel	441.46	2.2989	0.2537	181.81

Measurement instruments

In the laboratory experimental setup, K-type thermocouples are used for the outlet air temperature of the glass box (T_2), the outlet air temperature of the adsorbent bed (T_6), and outlet cooling water temperature (T_9) recorded by data logger with a resolution of 0.1 °C. The outlet air relative humidity of the glass box (RH_2) and adsorbent bed (RH_6) is measured by hygrometers, and airflow by an anemometer (V_3).

In the solar adsorption system, the outlet air temperature of the glass box (T_2), the outlet air temperature of ETC (T_5), and outlet cooling water temperature (T_8) are measured by K-type thermocouples and recorded by the data logger. The outlet air relative humidity of the glass box (RH_2) and adsorbent bed (RH_5) is measured by hygrometer, and airflow by an anemometer (V_3). It is worth mentioning that glass box outlet air is controlled automatically using a thermostat. The installation location of measuring instruments is shown in Fig. 1 and Fig. 2, and their specifications are listed in Table 3. In addition, the analysis of the inaccuracy of measuring instruments is given in Table 3. This analysis shows the expanded uncertainties with a confidence level of 95% to check the accuracy of the measurements (Faegh and Shafii 2017).

Result and discussion

The experiments in this study are divided into five case studies. The first four case studies are performed in a laboratory experimental setup. The assessment of the laboratory experimental setup is carried out three times for each test and the mean amount of water production is depicted in figures. The details of these experiments are explained as follows:

Table 3 The specification of measuring devices and inaccuracy analysis

Device type	Range	Calibration uncertainty	Resolution	Expanded uncertainty
1. Flow anemometer Smart sensor AR846	0.4–45 m/s	0.1	0.1	0.23 m/s
2. LCD digital thermometer/hygrometer LX8011	10–99%	1	1	2.3%
3. K-type thermocouple with Lutron BTM-4208sd Datalogger	−200–1250 °C	1	0.1	1.006 °C
4. Thermostat	0–100%	1	1	2.3%
	−40–99 °C	1	0.1	1.006 °C
5. Graduated cylinder	0–500 mL	–	5	5.8 mL
6. Pyranometer (SP-apogee sensor 110)	0–2000 W/m^2	5	1	10.06 W/m^2

Case study 1: Variable adsorption time

In the laboratory experimental setup, the amount of water produced in one adsorption–desorption cycle at different adsorption times with a constant desorption time of 1 h in the two adsorbents is compared. The default conditions in silica gel and hydrogel are as follows:

According to Table 4, T_2 and RH_2 are fixed at 40 °C and 90%, respectively. In this case study, the durations of the adsorption process are 2, 3, 4, 5, 6, and 7 h for silica gel, and for hydrogel they are 3, 4, 5, 6, and 7 h. The duration of the desorption process is considered to be 1 h.

As shown in Fig. 4, silica gel and hydrogel adsorb more moisture as the adsorption time increases. In this case study, as mentioned above, desorption duration is kept constant. Due to the properties of silica gel, as the adsorption time increases, the saturation state occurs (observed after 6 h onwards). The maximum water production using silica gel with 6 or more hours of adsorption time is 0.36 L/kg silica gel. On the other hand, the hydrogel does not include a saturation state in this experiment, and ultimately produces more water than silica gel. The highest amount of hydrogel productivity is 0.58 L/kg hydrogel with 7 h of adsorption time.

The outlet air relative humidity of the adsorbent bed (RH_6) in the test with 7-h adsorption time is shown in Fig. 5. At first, RH_6 is low in both experiments and indicates high moisture adsorption level in adsorbents. This amount increases over time, causing a decrease in moisture storage capacity and absorption by adsorbents. Silica gel is almost saturated after 6 h and the relative humidity of inlet air and outlet air of the adsorbent bed are the same. However, hydrogel can adsorb moisture even after 7 h following the adsorption process as the RH_6 is still much less than RH_2.

Table 4 Basic specifications of case studies for the laboratory experimental setup

RH_2	T_2	Weight	Mesh	V_3	Material
90%	40 °C	60 gr	2360 µm	3.4 m/s	Silica gel
90%	40 °C	12 gr	2000 µm	3.4 m/s	Hydrogel

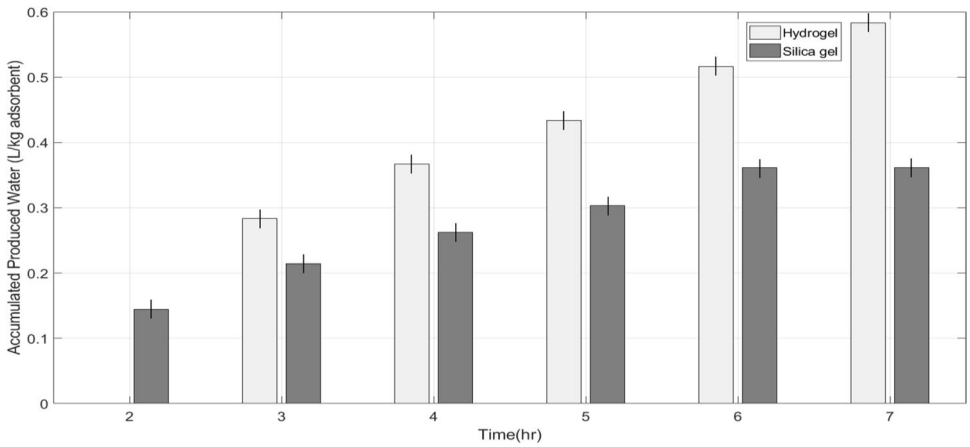

Fig. 4 Accumulated produced water in the first case study

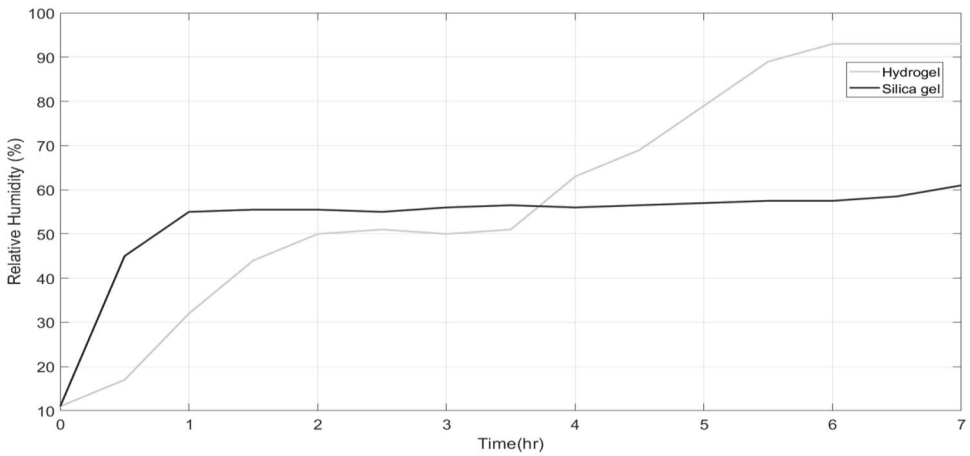

Fig. 5 The variation in RH_6 (the outlet air relative humidity of the adsorbent bed) for the test with 7-h adsorption time

Case study 2: Variable desorption time

In this case study, the adsorption process time is constant and carried out for 3 h and the desorption process time varies from 2 to 5 h for silica gel only. Table 5 provides the comparison between the accumulated water production using silica gel in the first and the second case studies.

Table 5 shows that if there is a 3-h adsorption process, a 3-h desorption process can extract about 97% of the moisture stored in silica gel. In addition, all of the moisture in silica gel can be extracted in about 4-h desorption time, the value of which according to Table 5 is 0.25 L/kg silica gel.

According to the results of the first case study on a 1-h desorption process, with an increase in the absorption time from 1 to 6 h, water production rises. After 6 h of adsorption, the produced water does not change due to the saturation of the silica gel, and the maximum amount of accumulated water production remains at 0.361 L/kg of silica gel. On the other hand, in case study 2, at a constant adsorption time of 3 h, the amount of produced water increases with a rise of up to 4 h in the desorption time, when the silica gel dries and the accumulated water production remains constant.

Table 5 Comparison results of the first and the second case studies for silica gel

Variable adsorption or desorption time	Accumulated water production (L/kg silica gel)	
	Variable adsorption time (case study 1)	Variable desorption time (case study 2)
	Constant desorption time (1 h)	Constant adsorption time (3 h)
2 h	0.144	0.188
3 h	0.214	0.244
4 h	0.262	0.251
5 h	0.303	0.251
6 h	0.361	–
7 h	0.361	–

Case study 3: Variable inlet air temperature and relative humidity

In the adsorption process of the third case study, RH_2 is chosen to be 50%, 70%, and 90%, and the T_2 is selected at 30° C, 40° C, and 50 °C. The durations of the adsorption and desorption processes are equally 30 min. Figure 6 indicates that by increasing RH_2 and T_2 in both silica gel and hydrogel, water production grows. The temperature increase leads to a rise in the amount of water vapor in the incoming air, resulting in more water being absorbed into both silica gel and hydrogel and more water being produced.

The results indicate that the highest water production in both hydrogel and silica gel occurs in RH_2 of 90% and T_2 of 50 °C, which is equal to 0.166 L/kg hydrogel and 0.116 L/kg silica gel, respectively. These indicate that this system is more suitable for hot and humid areas, in which more moisture is stored and consequently more freshwater can be produced. With a 20% increase in RH_2, the freshwater production of both silica gel and hydrogel rises, by about 57.11% and 82.35%, on average, respectively. In addition, with a 10 °C increase in T_2, more water is generated using both silica gel and hydrogel in this system, with a mean of 77.1% and 70.7%, respectively. Moreover, in hydrogel tests, at T_2 of 30, 40, and 50 °C, with a 20% increase in RH_2, productivity of freshwater increases by 103.7%, 93.6%, and 49.7%, respectively, and for silica gel, these values are 78.8%, 58.7%, and 33.7%, respectively. Therefore, it can be concluded that with an increase in temperature, the water vapor capacity of the inlet air entering the adsorbent material rises as well.

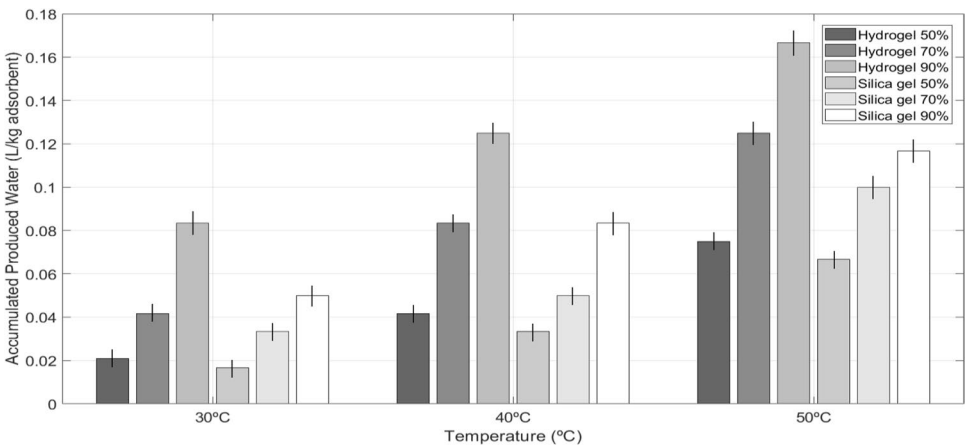

Fig. 6 Accumulated produced water of silica gel and hydrogel in the third case study

Case study 4: Variable mesh size

In this case study, V_3 is 1.7 m/s. Silica gel mesh sizes are 2360 µm and 850 µm, with hydrogel mesh sizes being 2000 µm and 650 µm. The adsorption and desorption processes are chosen to be equally 30 min each.

Comparing case study 4 with case study 3, it can be said that by reducing air velocity, V_3, from 3.4 to 1.7 m/s, the amount of water production of both hydrogel and silica gel decreases, by about 200.4% and 293.36%, respectively. According to Fig. 7, the highest water production of both silica gel and hydrogel occurs at smaller mesh sizes, which are 0.061 L/kg silica gel and 0.167 L/kg hydrogel, respectively. The results indicate that by changing the hydrogel mesh size from 2000 to 650 µm, more water is produced, about 301.4%. Water production of silica gel also increases by about 189.5% as the mesh size is changed from 2360 to 850 µm. In other words, it seems that the adsorption process is related to the mesh size of the adsorbent, and with decreasing the particle mesh size of silica gel and hydrogel, the amount of air moisture adsorption increases and, therefore, the amount of produced water under the same conditions, enhances. However, the number of tests with different mesh sizes in this study is not enough to make definite conclusions, and more experiments are needed in this regard. In addition, the effect of mesh size on the water production of hydrogel is much more than that of silica gel, and on the other hand, the V_3 changes in the silica gel have more effects on water production.

Case study 5: Variable inlet air temperature and relative humidity in solar-driven adsorption desalination system

In case study 5, the solar-driven adsorption desalination system is exposed to the sun for 8 h. As a result, the tests are performed in an 8-h adsorption process in the morning and an 8-h desorption process at night. In this system, by utilizing 1700 g of silica gel with a mesh size of 3000–5000 µm, four tests with different T_2 and RH_2 are conducted. The angle of the ETC with respect to the horizon of 70° is chosen to reduce sun irradiation on the ETC and its temperature. Tests 1 to 4 are performed from June 15 to June 18, 2019. In the adsorption process, the inlet air temperature of the tube is set at 30 and 40° C and its relative humidity RH_2 is adjusted to 70% and 90%. The solar irradiance on the ETC surface in terms of hours is shown in Fig. 8. As can be observed, the irradiances in these 4 tests are almost the same and as a result water production under the same conditions would be comparable. T_5 of the desorption process in the first test is depicted in Fig. 8. As can be seen, ETC temperature, T_5, rises to 120 °C in 5 h and then it decreases to 15 °C in 3 h in the afternoon as the solar irradiance decreases. In addition, the peak value of the T_5 which is 139.7 °C occurs at 14:00. The solar irradiance reaches its maximum value of 854.1 W/m^2 at around 13:00, after which the radiation intensity decreases and reaches 620.1 W/m^2 at 17:00.

Figure 9 displays the productivity of freshwater in four tests. Similar to the third case study, it is observed that with an increase in RH_2 and T_2, the water vapor capacity of the air also rises and therefore more moisture is absorbed by the silica gel and more water is produced in the desorption process. In addition, the maximum water production of silica gel occurs at RH_2 of 90% and T_2 of 40° C, which is equal to 1.518 kg/m^2 day, showing that the system is more suitable for hot and humid regions. Furthermore, with a 20% increase in RH_2, from 70 to 90%, the mean amount of water production of silica gel increases by 73.6%, compared to 58.7% in case study 3. Moreover, with a 10 °C increase in T_2 from 30 °C to 40 °C, silica gel produces more water with an average of 67.5%, compared to 58.7% in case study 3.

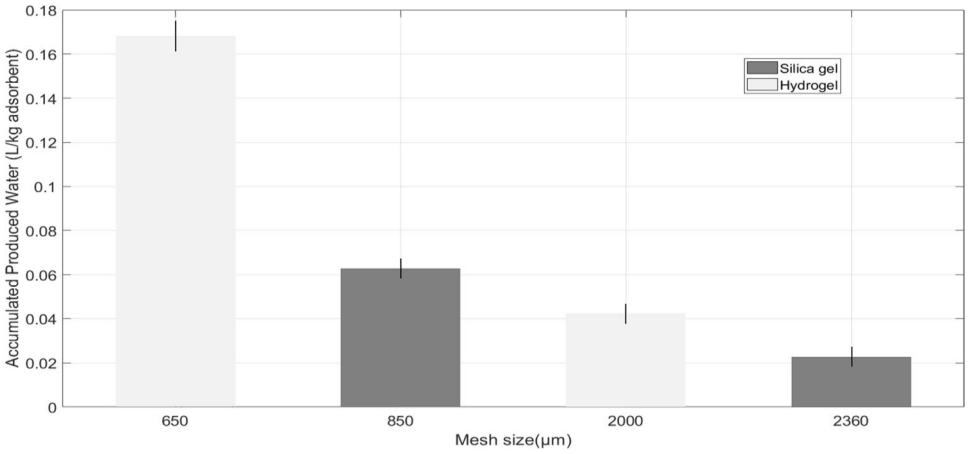

Fig. 7 Accumulated produced water at different mesh sizes in the fourth case study

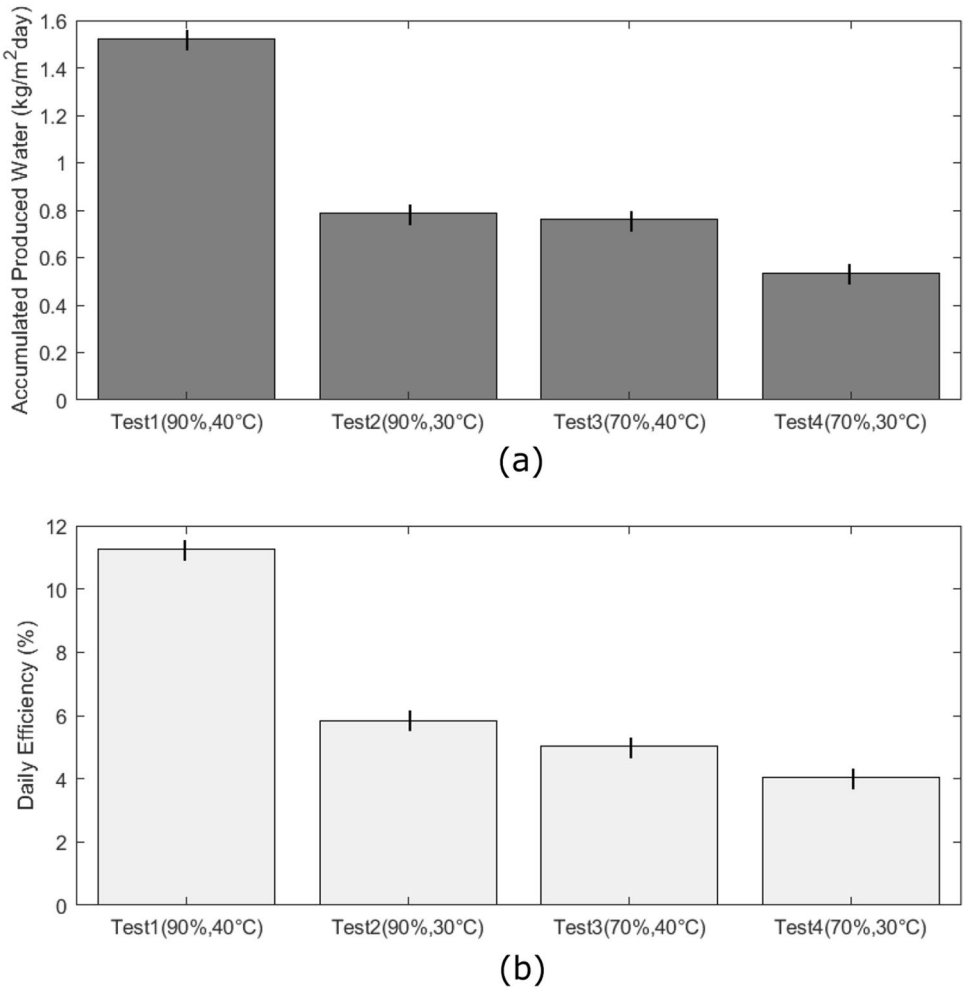

Fig. 8 The solar intensity in four tests on solar-driven adsorption desalination system and T_5 (the temperature of exhaust air from the ETC) variation in the desorption process of the first test

Methodology and data reduction

Daily efficiency

According to Abbaspour et al. (2019), the daily efficiency equation of the solar-driven adsorption desalination system can be expressed as:

$$\eta_d = \frac{\sum_t m \times h_{fg}}{\sum_t I(t) \times A + W_f + W_p} \quad (1)$$

in which $\dot{m}$, h_{fg}, A, $I(t)$, W_f, and W_{p} are mass flow rate of water production, latent heat of water evaporation, the collector area, the solar intensity, work of the fan, and work of the pump, respectively. As Fig. 9 illustrates, the daily efficiency of the first test of the solar-driven adsorption desalination system is 11.25%, which decreases with falling RH_2 and T_2 of all tests, the fourth one shows a daily efficiency of 4.06%. The low efficiency of this system appears to be due to the low temperature and low relative humidity of the inlet air. It is clear that if the relative humidity of the air entering the system is 0, the efficiency tends to be also 0 since neither moisture is adsorbed nor water is produced.

Thermodynamic analysis

According to Fig. 6 and calculation of absolute humidity inlet and outlet air of adsorbent bed using the psychrometric chart, the used silica gel adsorbent in this study adsorbs water vapor on average about 25% of its weight for an inlet air temperature of 40 °C and relative humidity of 90%. Therefore, for 1700 gr of silica gel, it is expected that about 425 gr of water is stored in silica gel during the adsorption process. On the other hand, it is observed that the produced water by this system in test 1 is equal to 157 gr (or 1.518 kg/m^2). The reason for this difference is the low efficiency of the used condenser; because according to Fig. 8, the temperature of the exhaust air from the ETC (T_5) reaches above 120 °C, and it is expected that the maximum amount of water stored in the silica gel to be extracted in the desorption process (Erkoc 2017). Due to the high amount of T_5, a large part of the vapors produced exit the condenser without changing

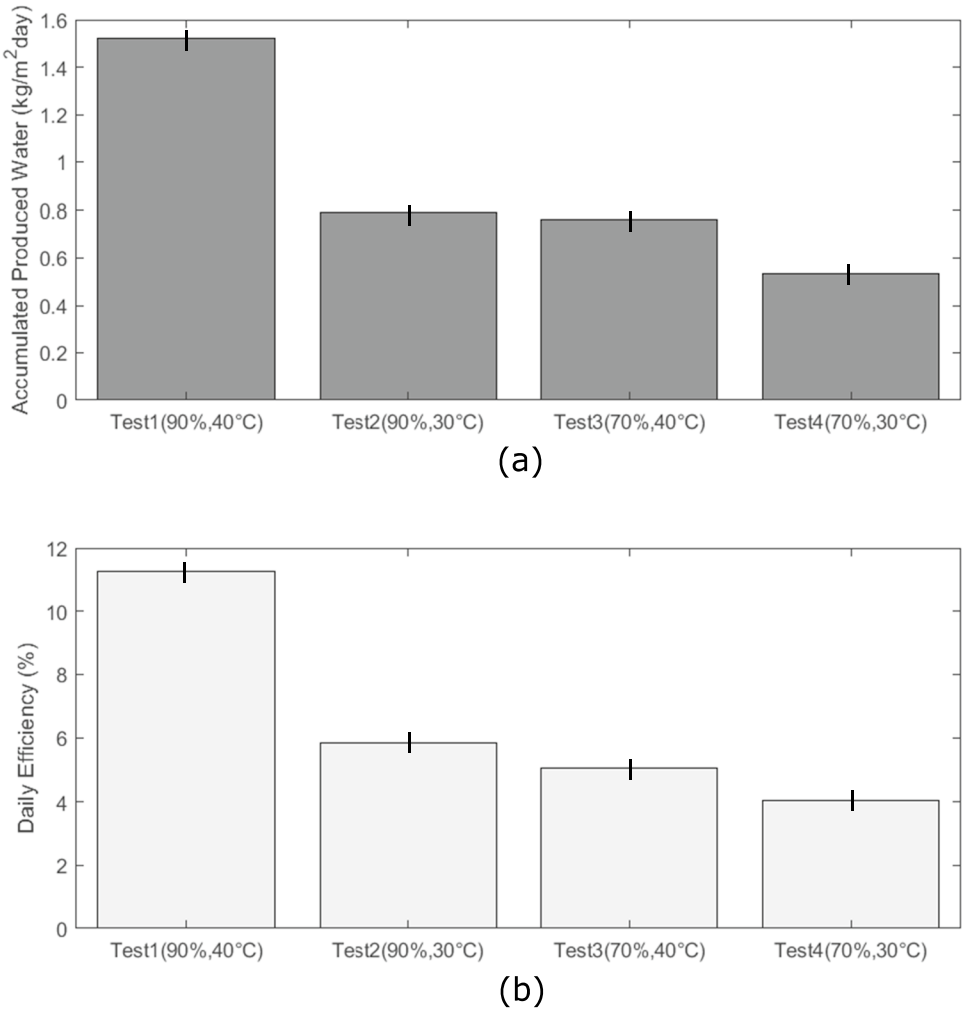

Fig. 9 **a** Accumulated water production and **b** the daily efficiency of solar-driven adsorption desalination system

the phase. To illustrate the point, at 11 o'clock in test 1, it was observed that T_5 and RH_5 in the desorption process were 70.2 °C and 100%, respectively. Then, as air passed through the condenser, its temperature reached 58.1 °C, while its relative humidity was still 100%. Considering the flow rate of the exhaust air and the humidity ratio before and after the condenser, about 49.28% of the formed vapor was wasted as exhausted without changing the phase and the rest was converted into fresh water. Had the condenser been ideal, the T_6 would have become equal to the temperature of the cooling fluid of the condenser (about 18 °C at 11 o'clock) and 95.32% of the vapors extracted from silica gel would have been converted into fresh water. Therefore, it is expected that with a better design of the condenser, the T_6 will approach the temperature of the cooling fluid and such a condenser will produce 405 g of freshwater, and the daily efficiency of the system will reach 29.02%.

According to Qiu et al. (2017), for complete drying of silica gel, these adsorbents should be exposed to air at 150 °C for 2 to 3 h, so that to extract 0.425 kg of water vapor per 1 kg of silica gel and 1394.8 kJ of thermal energy is required. In test 1 of the solar-driven adsorption desalination system, the amount of irradiance energy received by the ETC during the 8 h of test 1 is equivalent to 2532.5 kJ which is greater than the required thermal energy to extract the whole water stored in the silica gel adsorbents. Therefore, according to the mass of silica gel used in test 1 (1700 gr), for complete extraction of water, about 5 h of sunlight is required, which is consistent with the experimental results provided in Fig. 9. As a result, 32.8% of the solar energy irradiated on the vacuum tube is not used during the test from 2 pm onwards. If only the first 5 h of the desorption process are taken into account, the daily efficiency of the system in test 1 will become about 16.74%. In summary, by using an ideal condenser and increasing the mass of silica gel, the daily efficiency of the system for test 1 could reach 43.18%.

As was mentioned before, the angle of the ETC in this study is chosen at 70° with respect to the horizon to reduce sun irradiation on the ETC. On the other hand, according to Fig. 8, T_5 is higher than 120 °C in the afternoon and reaches a maximum of 140 °C at 14 o'clock. Therefore, it

is concluded that temperatures above 140 °C can also be achieved with this system (Kalogirou 2014). This high temperature is sufficient to completely dry the silica gel and prepare it for better use in the adsorption process, and this temperature also promises the use of high capacity adsorbents such as hydrogel or zeolite and can be used to achieve more water production and increase the system's daily efficiency.

Economic analysis

The economic analysis of the solar-driven adsorption desalination system is done as well. Table 6 lists the necessary economic parameters of the first test of the solar-driven adsorption desalination system (Ali et al. 2021). As can be seen, the CPL of the first test with the most productivity is 0.0699 $/L, which can be reduced if better adsorbent materials are utilized.

The accumulated water production of the present work on a daily basis is shown in Fig. 9. The accumulated water production of the first test, with the highest amount of water production, is compared to the previous studies in Table 7.

It is worth noting that the current study produces more accumulated water on a daily basis than different solar-driven adsorption desalination systems and this shows that utilizing silica gel with ETC is feasible. As a future study, the transient behavior of the solar desalination system can be predicted using meta-heuristic algorithms in different initial conditions (Ebrahimpour et al. 2021). Additionally, using semi-analytical approaches, the amount of water produced by the system can be estimated in different modes (Mishra et al. 2021).

Conclusion

In this study, a novel automatic irrigation system is designed and built as a solar-driven adsorption desalination system with an ETC filled with silica gel. During the night, the system adsorbs and stores air moisture by means of adsorbent materials, and during the day, the desorption process occurs in the presence of sunlight. An ETC has to be used

Table 6 Economic analysis for solar-driven adsorption desalination system

Parameters	Unit	Test1(Solar)
Principle cost (*P*)	$	30.28
Salvage value (*S*) (10% of principal value)	$	3.028
Life of the system (*n*)	Yrs	20
Interest rate (*i*)	%	10
Capital recovery factor (CRF)	–	0.117
Sink fund factor (SFF)	–	0.017
Annual first cost (CRF × *P*)	$	3.542
Annual salvage value (SFF × *S*)	$	0.051
Annual maintenance cost (0.15 annual first cost)	$	0.531
Annual cost = (Annual first cost + annual maintenance cost − annual salvage value)	$	4.022
Average daily accumulated water production (ADAWP)	kg/m^2	1.518
Annual accumulated water production of the system (ADAWP × 365)	kg/m^2	554.07
Annual useful energy (annual accumulated water production × latent heat of vaporization (= 0.65 kWh/kg))	kWh/m^2	360.145
Annual cost of produced water per kg (annual first cost/annual accumulated water production)	$	0.0064
Annual cost of produced water per kWh (annual first cost/annual useful energy)	$	0.0098
Cost per liter (CPL = Annual cost/Annual accumulated water production of system)	$/L	0.0699
Cost per liter per unit area of system (Annual cost/Annual accumulated water production of system)	$/L/m^2	0.0073

Table 7 Comparison of maximum daily accumulated water production for different AD systems

	Experiment	System description	Type of study	Adsorbent	Daily accumulated water production (kg/m^2 day)
1	Essa et al. (2020)	Double-slope half-cylindrical basin solar still (DS-HCBSS)	Exp	Silica gel	0.150
2	Essa et al. (2020)	DS-HCBSS + Fins	Exp	Silica gel	0.258
3	Essa et al. (2020)	DS-HCBSS + Fins + Gravel	Exp	Silica gel	0.400
4	**Present study**	ADS with ETC	Exp	Silica gel	1.518

in this system because it reaches a higher temperature in the desorption process and as a result more water is produced. In addition, in the laboratory experimental setup, the performance of silica gel and hydrogel adsorbents in terms of water production is compared to changing various input parameters such as inlet air humidity, inlet air temperature, and adsorption and desorption processing time. The following results are concluded:

- At variable adsorption time of the laboratory experimental setup, the highest productivity of freshwater using silica gel and hydrogel is 0.36 L/kg silica gel and 0.58 L/kg hydrogel, respectively, which occurs during the adsorption time of 7 h.
- All of the moisture in silica gel is extracted within the first four hours of desorption time, whose value is 0.25 L/kg silica gel at variable desorption time.
- According to the result of variable inlet air temperature and relative humidity of the laboratory experimental setup, the highest water production of hydrogel and silica gel occurs at the inlet air relative humidity of 90% and temperature of 50 °C, with 0.166 L/kg hydrogel and 0.116 L/kg silica gel, respectively.
- At variable adsorbent mesh sizes, the highest amount of water is produced for silica gel and hydrogel at smaller mesh sizes, 850 µm and 650 µm respectively. The highest water production amount is for 0.061 L/kg silica gel and 0.167 L/kg hydrogel.
- By reducing air velocity from 3.4 to 1.7 m/s, water production for hydrogel and silica gel decreases by about 200.4% and 293.36%, respectively.
- The maximum daily efficiency and accumulated daily water production of the novel solar-driven adsorption desalination system are 11.25% and 1.518 kg/m^2 day, respectively. The results indicate that this system can be used as an automatic farm irrigation system in hot and humid areas. The CPL of this novel system is calculated to be 0.0699 $/L.

Nomenclature

$\boldsymbol{A}$ [m^2]: The collector area; C_a [L/kg]: The adsorption isotherm capacity in liter per kilo gram of adsorbent; $\boldsymbol{h_{fg}}$ [J/kg]: Latent heat of water evaporation; $\boldsymbol{I(t)}$[W/m^2]: The solar intensity; $\boldsymbol{\dot{m}}$ [kg/s]: Mass of water production flow rate; P [kPa]: Pressure; T [°C]: Temperature; W [W]: Work

Subscript

f: Fan; p: Pump

Acronyms

AD: Adsorption desalination; ADS: Adsorption desalination system; COP: Coefficient of performance; CPL : Coefficient of performance; CPL : Cost per liter; ETC: Evacuated tube collector; FO: Forward osmosis; GOR: Gain output ratio; HDH: Humidification-dehumidification; RH : Reverse Osmosis; RO: Reverse osmosis; RR: Recovery ratio

Acknowledgements The authors want to express their gratitude to the Deputy of Research and Technology of Sharif University of Technology and Sharif Energy, Water and Environment Institute (SEWEI) for providing a suitable working environment to carry out the experiments.

Author contribution MZS and MBS contributed to the conceptualization, methodology, and design of this study. MZS and BE also contributed to the investigation, data curation, resources, and writing-original draft. BE and MBS did writing review & editing together. BE analyzed data and contributed to the validation of data. MBS was the supervision of this study. All authors read and approved the final manuscript.

Data availability The datasets used and/or analyzed during the current study are available from the corresponding author on reasonable request.

Declarations

Ethics approval Not applicable.

Consent to participate Not applicable.

Consent to publish Not applicable.

Conflict of interest The authors declare no competing interests.

References

Abbaspour MJ, Faegh M, Shafii MB (2019) Experimental examination of a natural vacuum desalination system integrated with evacuated tube collectors. Desalination 467:79–85. https://doi.org/10.1016/j.desal.2019.06.004

A Akbar et al 2019 A review on the water-energy nexus for drinking water production from humid air Renewable and Sustainable Energy Reviews (nov) https://doi.org/10.1016/j.rser.2019.109627

Ali ES et al (2017) Weather effect on a solar powered hybrid adsorption desalination-cooling system: a case study of Egypt's climate. Appl Therm Eng 124:663–672. https://doi.org/10.1016/j.applthermaleng.2017.06.048

Ali HM, Arif S, Theppaya T (2021) Techno economic evaluation and feasibility analysis of a hybrid net zero energy building in Pakistan: a case study of hospital. Frontiers in Energy Research 9:127. https://doi.org/10.3389/fenrg.2021.668908

AS Alsaman et al 2017 Performance evaluation of a solar-driven adsorption desalination-cooling system Energy https://doi.org/10.1016/j.energy.2017.04.010

A Amirfakhraei T Zarei J Khorshidi 2020 Performance improvement of adsorption desalination system by applying mass and heat recovery processes Thermal Sci and Eng Progress https://doi.org/10.1016/j.tsep.2020.100516

Ashraf S et al (2021) Recent progress on water vapor adsorption equilibrium by metal-organic frameworks for heat transformation

applications. Int Commun Heat Mass Transfer 124:105242. https://doi.org/10.1016/j.icheatmasstransfer.2021.105242
Capocelli M et al (2018) Process analysis of a novel humidification-dehumidification-adsorption (HDHA) desalination method. Desalination 429:155–166. https://doi.org/10.1016/j.desal.2017.12.020
Du B et al (2017) Area optimization of solar collectors for adsorption desalination. Sol Energy 157:298–308. https://doi.org/10.1016/j.solener.2017.08.032
Ebrahimpour B et al (2021) Enhancing performance of an air conditioner by preheating and precooling of liquid desiccant and non-processed air. Int J Eng Trans B Appl 35(2):425–432. https://doi.org/10.5829/ije.2022.35.02b.19
Elbassoussi MH, Mohammed RH and Zubair SM (2020) Thermo-economic assessment of an adsorption cooling/desalination cycle coupled with a water-heated humidification-dehumidification desalination unit. Energy Conversion and Management 223(August). https://doi.org/10.1016/j.enconman.2020.113270
Erkoc P (2017) Design of biodegradable hydrogels for the development of in vitro models for Glioblastoma Multiforme. Koc University. https://doi.org/10.13140/RG.2.2.17618.45761
Essa FA et al. (2020) Extracting water content from the ambient air in a double-slope half- cylindrical basin solar still using silica gel under Egyptian conditions. Sustainable Energy Technologies and Assessments 39(Feb). https://doi.org/10.1016/j.seta.2020.100712
Faegh M, Shafii MB (2017) Experimental investigation of a solar still equipped with an external heat storage system using phase change materials and heat pipes. Desalination 409:128–135. https://doi.org/10.1016/j.desal.2017.01.023
Jamil F, Ali HM (2019) Sustainable desalination using portable devices: a concise review. Sol Energy 194:815–839. https://doi.org/10.1016/j.solener.2019.10.085
Ji JG, Wang RZ, Li LX (2007) New composite adsorbent for solar-driven fresh water production from the atmosphere. Desalination 212:176–182. https://doi.org/10.1016/j.desal.2006.10.008
Kabeel AE, Abdelgaied M (2019) A new configuration of the desiccant dehumidifier with cut-segmental silica-gel baffles and water cooling for air conditioning coupled with HDH desalination system. Int J Refrig. https://doi.org/10.1016/j.ijrefrig.2019.04.009
Kabeel AE, Abdelgaied M, Zakaria Y (2017) Performance evaluation of a solar energy assisted hybrid desiccant air conditioner integrated with HDH desalination system. Energy Convers Manage 150:382–391. https://doi.org/10.1016/j.enconman.2017.08.032
Kalogirou SA (2014) Solar energy engineering processes and systems Second Edition. Academic Press (Elsevier).
Khalid SU et al (2021) Heat pipes: progress in thermal performance enhancement for microelectronics. J Therm Anal Calorim 143(3):2227–2243. https://doi.org/10.1007/s10973-020-09820-7
Mishra SR, Mathur P, Ali HM (2021) Analysis of homogeneous–heterogeneous reactions in a micropolar nanofluid past a nonlinear stretching surface: semi-analytical approach. J Therm Anal Calorim 144(6):2247–2257. https://doi.org/10.1007/s10973-020-10414-6
Mitra S et al (2014) Solar driven adsorption desalination system. Energy Procedia 49:2261–2269. https://doi.org/10.1016/j.egypro.2014.03.239
Mittal H, Alili A and Alhassan SM (2020) Adsorption isotherm and kinetics of water vapors on novel superporous hydrogel composites. Microporous and Mesoporous Materials. https://doi.org/10.1016/j.micromeso.2020.110106
Mohammed RH et al (2018) Physical properties and adsorption kinetics of silica-gel/water for adsorption chillers. Appl Therm Eng 137:368–376. https://doi.org/10.1016/j.applthermaleng.2018.03.088
Mortimer EC (1983) *Chemistry fifth edition*. Wadsworth Publishing Company.
Qasem NAA, Zubair SM (2019) Performance evaluation of a novel hybrid humidification-dehumidification (air-heated) system with an adsorption desalination system. Desalination 461:37–54. https://doi.org/10.1016/j.desal.2019.03.011
Qiu Y et al. (2017) Developing solid oral dosage forms Pharmaceutical Theory & Practice.
Z Rahimi-ahar MS Hatamipour L Rahimi Ahar 2020 Air humidification-dehumidification process for desalination: a review Prog Energy Combust Sci 80 https://doi.org/10.1016/j.pecs.2020.100850
Rezk H et al (2019) Identifying optimal operating conditions of solar-driven silica gel based adsorption desalination cooling system via modern optimization. Sol Energy 181:475–489. https://doi.org/10.1016/j.solener.2019.02.024
Sadri S, Ameri M, Khoshkhoo RH (2018) A new approach to thermo-economic modeling of adsorption desalination system. Desalination 428:69–75. https://doi.org/10.1016/j.desal.2017.11.027
AA Salehi et al 2020 Hydrogel materials as an emerging platform for desalination and the production of purified water Sep Purif Rev 1–20 https://doi.org/10.1080/15422119.2020.1789659
Suleimenov I et al (2017) New desalination systems based on thermo-sensitive hydrogels. J Int Sci Publications 11:129–137
Talaat MA et al (2018) Solar-powered portable apparatus for extracting water from air using desiccant solution. Renewable Energy 119:662–674. https://doi.org/10.1016/j.renene.2017.12.050
Wang X, Ng KC (2005) Experimental investigation of an adsorption desalination plant using low-temperature waste heat. Appl Therm Eng 25:2780–2789. https://doi.org/10.1016/j.applthermaleng.2005.02.011
Youssef G, Mahmoud SM, Al-dadah RK (2015) Seawater desalination technologies. Int J Innov Sci and Res 4:402–422
Youssef PG, Al-dadah RK, Mahmoud SM (2014) Comparative analysis of desalination technologies. Energy Procedia 61:2604–2607. https://doi.org/10.1016/j.egypro.2014.12.258